catalysts

MDPI

Article

Photoelectrochemical Oxidation in Ambient Conditions Using Earth-Abundant Hematite Anode: A Green Route for the Synthesis of Biobased Polymer Building Blocks

Anurag Kawde [1,2,*,†], Mahmoud Sayed [3,4,†], Qi Shi [2], Jens Uhlig [1,2], Tönu Pullerits [2,*] and Rajni Hatti-Kaul [3,*,‡]

[1] Lund Institute of Advanced Neutron and X-ray Science, Lund University, P.O. Box 124, SE-22100 Lund, Sweden; Jens.uhlig@chemphys.lu.se
[2] Chemical Physics and NanoLund, Department of Chemistry, Lund University, P.O. Box 124, SE-22100 Lund, Sweden; qi.shi@chemphys.lu.se
[3] Division of Biotechnology, Department of Chemistry, Lund University, P.O. Box 124, SE-22100 Lund, Sweden; mahmoud.sayed_ali_sayed@biotek.lu.se
[4] Department of Botany and Microbiology, Faculty of Science, South Valley University, Qena 83523, Egypt
* Correspondence: anurag.kawde@linxs.lu.se (A.K.); tonu.pullerits@chemphys.lu.se (T.P.); rajni.hatti-kaul@biotek.lu.se (R.H.-K.)
† Authors contributed equally.
‡ Lead Contact.

Abstract: This study demonstrates the use of a photoelectrochemical device comprising earth-abundant hematite photoanode for the oxidation of 5-hydroxymethylfurfural (5-HMF), a versatile bio-based platform chemical, under ambient conditions in the presence of an electron mediator. The results obtained in this study showed that the hematite photoanode, upon doping with fluorine, can oxidize water even at lower pH (4.5 and 9.0). For 5-HMF oxidation, three different pH conditions were investigated, and complete oxidation to 2,5-furandicarboxylic acid (FDCA) via 5-hydroxymethyl-2-furancarboxylic acid (HMFCA) was achieved at pH above 12. At lower pH, the oxidation followed another route via 2,5-diformylfuran (DFF), yielding 5-formyl-2-furancarboxylic acid (FFCA) as the main product. Using the oxidized intermediates as substrates showed DFF to be most efficiently oxidized to FDCA. We also show that, at pH 4.5, the addition of the laccase enzyme promoted the oxidation of 5-HMF to FFCA.

Keywords: photoelectrochemical cell; earth-abundant hematite photoanode; bio-based chemicals; 5-HMF oxidation; 2,5-furandicarboxylic acid

Citation: Kawde, A.; Sayed, M.; Shi, Q.; Uhlig, J.; Pullerits, T.; Hatti-Kaul, R. Photoelectrochemical Oxidation in Ambient Conditions Using Earth-Abundant Hematite Anode: A Green Route for the Synthesis of Biobased Polymer Building Blocks. *Catalysts* **2021**, *11*, 969. https://doi.org/10.3390/catal11080969

Academic Editor: Carlo Santoro

Received: 26 June 2021
Accepted: 12 August 2021
Published: 13 August 2021

1. Introduction

The tremendous growth in the chemical manufacturing industry during the past century has relied heavily on exploiting fossil resources to provide both carbon for the chemicals and materials as well as energy for the processes. The chemical manufacturing contributes nearly 20% of the global greenhouse gas emissions (amounting to 880 Mt CO_2 equivalent in 2018) [1,2]. Replacing fossil energy with a renewable alternative such as solar energy and using biomass for providing renewable carbon provides a sustainable route for a fossil-free chemical industry of the future [3–5]. In general, high energetic compounds are an excellent way to store harvested solar energy without the drawback of battery technology and are the basic idea behind photoelectrochemical cells (PECs) [3]. In a typical PEC operation, water is oxidized ($2H_2O \rightarrow O_2 + 4H^+$) at the semiconductor photoanode, while the protons liberated in this reaction migrate to the cathode to conduct a reduction reaction ($4H^+ + 4e^- \rightarrow 2H_2$) [6,7]. The produced H_2 is the significant energetic product stored for further use, and the second product, O_2, is of low industrial value [3,5]. An alternative oxidation reaction that produces instead high-value chemicals at the photoanode [8] could

significantly increase the fraction of stored energy as well as the efficiency of the system. The design criteria of such photoelectrodes are earth-abundant materials such as Si [9,10], Fe_2O_3 [11], CuO_2 [12], or $BiVO_4$ [13] that further reduce the cost and increase the scalability of the system, hence improving the cost–benefit ratio.

The reaction that has attracted considerable interest to replace water oxidation (O_2 production) in recent years is the oxidation of 5-hydroxymethylfurfural (5-HMF) to 2,5-furandicarboxylic acid (FDCA). The U.S. Department of Energy (DOE) has ranked 5-HMF and FDCA among the top value-added biomass-based chemicals [14]. While 5-HMF constitutes an essential platform for a large number of chemicals, including fuels, solvents, and polymer building blocks [15], FDCA is regarded as a sustainable alternative to terephthalic acid in the production of polyester polyethylene 2,5-furandicarboxylate (PEF) with better thermomechanical and barrier properties than polyethylene terephthalate (PET) [16]. FDCA is produced from 5-HMF through three oxidation steps, which can take two different routes, as shown in Scheme 1. Oxidation of 5-HMF has been reported using chemical [17,18], biocatalytic [19], electrochemical [20], or photoelectrochemical catalysis [5].

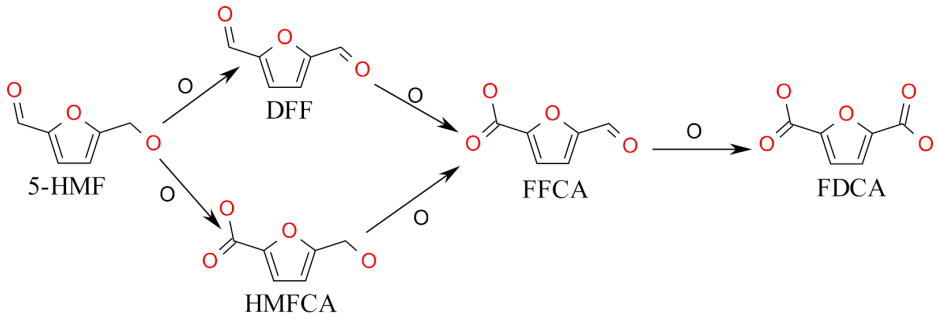

Scheme 1. Two possible pathways for oxidation of 5-HMF. The intermediates produced during the oxidation are as follows: 2,5-diformylfuran (DFF), 5-hydroxymethyl-2-furan-carboxylic acid (HMFCA), and 5-formyl-2-furoic acid (FFCA).

Earlier reports on the electrochemical oxidation of 5-HMF have indicated the need for large electroactive surfaces and high catalyst loadings to obtain high reaction rates and selective formation of FDCA [20]. A photoelectrochemical (PEC) system that utilizes solar energy for oxidation can be one of the most lucrative and clean options [21,22]. Photoinduced electron-hole pairs are generated at the valence band of the photoanode, and while the electrons are transferred to the cathode, the holes can be utilized at the anode for the oxidation reaction [3]. In the past few years, various studies using earth-abundant photoelectrodes/catalysts for the oxidation of 5-HMF have been reported using varying illumination intensities and varying 5-HMF concentrations [5,19,23]. Moreover, most of these systems have been operated at elevated temperatures. For the practical application of a system driven by solar light, it needs to work at a maximum of 100 mW/cm^2, which is the power density of a typical solar illumination at airmass filter of 1.5 G observed on the Earth [24]. Moreover, using as high a 5-HMF concentration as possible decreases the cost of product recovery from the reaction. Herein, we report the use of earth-abundant hematite photoanode for the PEC conversion of 5-HMF under ambient conditions of temperature (21 °C) and pressure, as well as different pH values.

2. Results and Discussion

2.1. Photolectrochemical Water Oxidation Using Hematite Nanorods

The (photo-)electrochemical oxidation is typically performed under alkaline conditions at which 5-HMF is prone to degradation into humin products [25]. On the other hand, the hematite surface is spontaneously corroded by the protons in the electrolyte in acidic or neutral conditions [26]. Thus, we tested the hematite photoanode performance at three different pH conditions (4.5, 9.0, and 12.5) first for water oxidation followed by

5-HMF oxidation. The hematite photoanode was synthesized on the conductive fluorine tin oxide (FTO) substrate to yield FTO/α-Fe_2O_3 following the method reported by Vayssieres et al. [27]. The FTO/α-Fe_2O_3 (bare hematite) was further modified by soaking in the fluoride-rich iron-oxide electrolyte (1 mM NH_4F in 0.15 M $FeCl_3$) to yield fluorine-doped FTO/α-Fe_2O_3/FeOOH (modified hematite) photoelectrode (see the Experimental section for detailed synthesis method). The morphological characterization (X-ray diffraction and scanning electron micrograph) of the photoelectrode is presented in Figure S1. The XRD (Figure S1a) for the bare and modified hematite overlaps for most phases except for the presence of a small distinctive peak at 23.8 deg, indicating the (110) phase of FeOOH. Figure S1b,c show the planar top view of the bare and modified hematite photoanode wherein the modified hematite shows a thin film formed on top of bare hematite.

The photoelectrode was placed in a photoelectrochemical cell. The net photocurrent density (photocurrent-dark current) J_{ph} was recorded at 1.23 V_{RHE} (voltage vs. reversible hydrogen electrode) for the bare hematite photoelectrode at pH 4.5, 9.0, and 12.5, giving 0.05, 0.1, and 0.48 mA/cm^2, respectively (Figure 1 dark gray color bar). The respective current–potential curves are shown in Figure S2a,b. Upon doping with fluorine, the J_{ph} at 1.23 V_{RHE} for the modified hematite photoelectrode increased significantly to 0.1, 0.16, and 1.18 mA/cm^2 at pH 4.5, 9.0, and 12.5, respectively (Figure 1 wine color bar), indicating the PEC performance of the α-Fe_2O_3 photoanode to be enhanced when functionalized with F-doped FeOOH. The effect is attributed to the reduced recombination losses at the surface of the α-Fe_2O_3 nanorods and enhanced charge transfer through the FeOOH, consistent with recent reports on F-doped hematite for water oxidation [28,29]. Thus, the F-doped FeOOH avoids the corrosion of the hematite electrode surface and enhances charge transfer even in mildly acidic electrolytes.

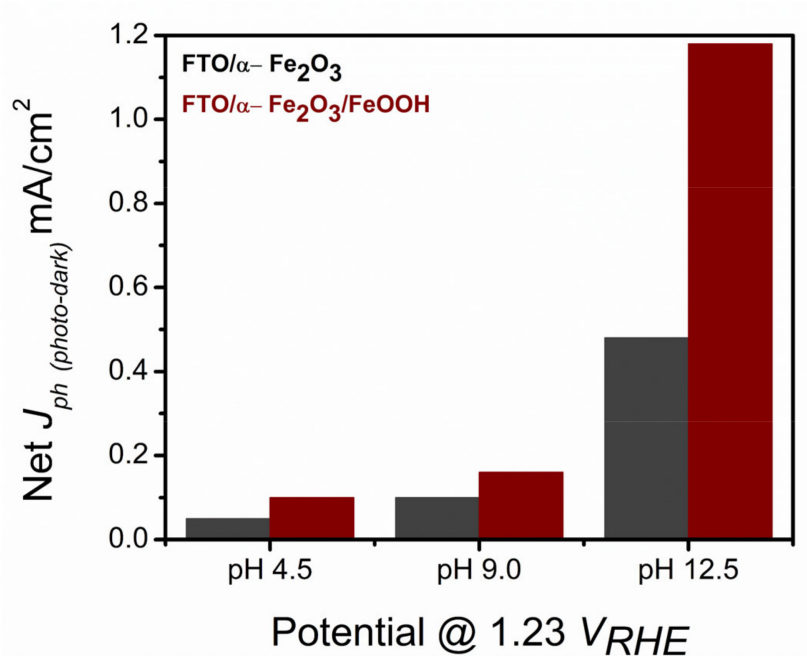

Figure 1. Net photocurrent responses for bare and modified hematite photoanodes for water oxidation at 1.23 V_{RHE}.

2.2. Photolectrochemical 5-HMF Oxidation

Subsequently, we evaluated the PEC performance of the modified hematite photoelectrode for the oxidation of 5-HMF, which was produced from fructose, using the method adopted from our previous study [30]. Figure 2a shows the current potential curves recorded for 5-HMF oxidation at pH 12.5 in 1 M Na_2SO_4, and the corresponding chronoamperometry (CA) response (Figure 2b) recorded at 1.1 VRHE. Interestingly, we found that the onset potential (V_{onset}) [10], defined here as the potential at which net

photocurrent density (J_{ph}) reaches 0.1 mA/cm^2, decreases by 30 mV from 0.81 to 0.78 V_{RHE} in the presence of 10 mM 5-HMF. This indicates that the oxidation of 5-HMF is favored over water oxidation. Additionally, J_{ph} of 1.8 mA/cm^2 was recorded for modified hematite at 1.4 V_{RHE}, which is 64% higher than that without 5-HMF. Similarly, the onset potential further decreases with the addition of 2,2,6,6-tetramethyl piperidine-1-yl)oxidanyl (TEMPO), a well-known artificial electron mediator [31]. Addition of 1 mg/mL and 2 mg/mL of TEMPO (6.4 mM and 12.8 mM) in the 10 mM 5-HMF solution decreases the V_{onset} by 90 mV to 0.72 V_{RHE} and by 220 mV to 0.59 V_{RHE}, respectively, indicating that the oxidation of TEMPO is significantly favorable over that of 5-HMF (see Table S1 for a summary). The addition of TEMPO decreased the V_{onset} and led to a phenomenal increase in the PEC performance of the 5-HMF oxidation system. We recorded the J_{ph} of 3.2 mA/cm^2 at 1.4 V_{RHE} for 1 mg/mL TEMPO that increased by more than a factor 2 to 7.8 mA/cm^2 on doubling the mediator concentration. TEMPO takes the photogenerated holes from α-Fe_2O_3-FeOOH and is oxidized to $TEMPO^+$ (oxo cation), which in turn oxidizes 5-HMF while simultaneously regenerating the TEMPO. Our observations agree with Cha and Choi [5] in that the shift (decrease) in the anodic onset potential by the addition of TEMPO significantly reduces the overpotential for 5-HMF oxidation without competing with water oxidation. As evident from Figure 2b, the photocurrent reaches a plateau after 3 h of CA, indicating that most of the 5-HMF is oxidized. The details of 5-HMF conversion under different conditions are given in Table 1.

Table 1. Photoelectrochemical oxidation of 5-HMF and derivatives using hematite photoanode at 20 °C and different pH values.

Experiment pH 12.5								
Experiment at 1.1 V_{RHE}	**5-HMF Conversion (%)**	**Time (h)**	**Product Profile (Selectivity %)**				**pH**	
			5-HMFCA	**DFF**	**FFCA**	**FDCA**	**Start**	**End**
10 mM 5-HMF	11.7	20	83.9	7.8	6.4	1.8	12.5	10
10 mM 5-HMF + 1 mg/mL TEMPO	42	20	71.1	1.4	4.1	23.4	12.5	11
10 mM 5-HMF + 2 mg/mL TEMPO	96.6	2.5	0.4	0.3	18.4	80.9	12.5	11
10 mM 5-HMF + 2 mg/mL TEMPO	99.2	5.5	0.5	2.2	6.4	90.7	12.5	11
Experiment pH 9.0								
Experiment at 1.1 V_{RHE}	**Conversion (%)**	**Time (h)**	**Product profile (Selectivity %)**				**pH**	
			5-HMFCA	**DFF**	**FFCA**	**FDCA**	**Start**	**End**
10 mM 5-HMF + 2 mg/mL TEMPO	47.3	20	1.5	31.7	66.2	1.6	9.0	5
10 mM 5-HMFCA + 2 mg/mL TEMPO	50.9	20	-	-	5.7	94.2	9.0	6
10 mM DFF + 2 mg/mL TEMPO	90.1	20	-	-	96.1	2.6	9.0	5
10 mM FFCA + 2 mg/mL TEMPO	40.6	20	-	-	-	97.4	9.0	5
Experiment pH 4.5								
Experiment at 1.1 V_{RHE}	**Conversion (%)**	**Time (h)**	**Product profile (Selectivity %)**				**pH**	
			5-HMFCA	**DFF**	**FFCA**	**FDCA**	**Start**	**End**
10 mM 5-HMF + 2 mg/mL TEMPO	51.7	20	1.6	29.6	67.3	1.5	4.5	4
10 mM 5-HMF + 0.5 mg/mL Laccase	14.9	20	21.4	53.5	24.1	1.0	4.5	4
10 mM 5-HMF + 2 mg/mL TEMPO + 0.5 mg/mL Laccase	78.3	20	0.7	7.7	85.9	5.7	4.5	4

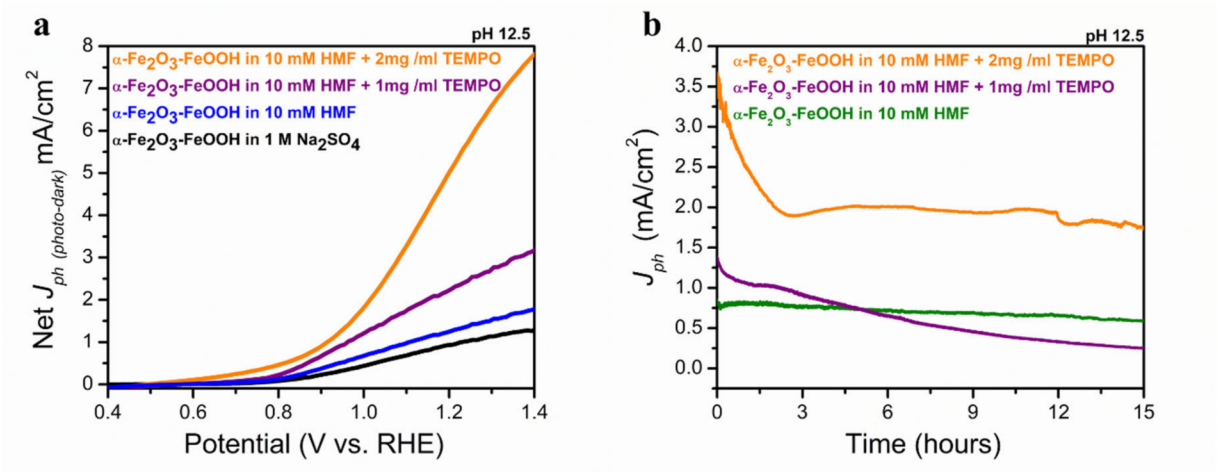

Figure 2. (**a**) Net photocurrent responses for 5-HMF photooxidation at pH 12.5 and (**b**) corresponding chronoamperometry (CA) response at 1.1 V_{RHE}.

Based on the decreased V_{onset} and higher J_{ph} obtained at 2 mg/mL of TEMPO, we performed PEC oxidation of 5-HMF at pH 9.0 and 4.5. Figure 3a,b show the current potential curves recorded at the two pH values; the V_{onset} followed a similar trend at pH 9.0 and 4.5 as at pH 12.5. The V_{onset} decreased by 410 mV in the presence of 5-HMF and was further reduced by 230 mV upon the addition of TEMPO. Likewise, the J_{ph} at 1.4 V_{RHE} was increased by more than a factor of 2 in the presence of 5-HMF and by almost a factor of 7 upon the addition of TEMPO. At pH 4.5, the V_{onset} reduced significantly by 390 mV in the presence of 5-HMF and by 720 mV by further addition of TEMPO. Similarly, almost a factor of 2 and 11 increase in J_{ph} was recorded at 1.4 V_{RHE} in the presence of 5-HMF and upon further addition of TEMPO, respectively. As the hematite bandgap is 2.1 eV (valence-band edge at ~2.3 V vs. RHE) [8,32], the photogenerated holes in the hematite have sufficient potential to oxidize TEMPO. Thus, the additional bias potential enhances electron–hole separation, increasing the oxidation at the photoanode surface [33]. According to cyclic voltammetry of TEMPO performed in an earlier report [34], the reversible electrochemical oxidation of TEMPO is insensitive to pH and the nature of the buffer used. The cyclic voltammograms for the oxidation of 5-HMF in dark and under illumination performed in this study are presented in Figure S3, indicating a typical redox behavior of TEMPO under different pH conditions.

These observations confirmed that the modified hematite photoanode can work efficiently for 5-HMF oxidation at different pH values in the presence of a mediator without interfering with the water oxidation reaction. The products formed during photoelectrochemical oxidation of 5-HMF under different conditions at pH 4.5, 9.0, and 12.5, respectively, are presented in Table 1. The corresponding chronoamperometry (CA) response recorded at 1.1 V_{RHE} is shown in Figure 2b and the Supplementary Materials (Figures S4 and S5a). We observed the 5-HMF photooxidation to be highly pH-dependent, in agreement with the earlier study [19]. Control measurements performed in the dark at different pH values did not show any detectable oxidation of 5-HMF (data not shown). As shown in Table 1, we achieved only 11.7% photoconversion of 5-HMF at pH 12.5 without a mediator; the significant fraction (83.9%) was converted to 5-hydroxymethyl-2-furancarboxylic acid (HMFCA), and the pH of the solution decreased to 10 at the end of the 20 h CA run. Supplementation of 1 mg/mL TEMPO resulted in 42% of 5-HMF being oxidized, of which 23.4% was FDCA and the remaining HMFCA, suggesting that oxidation occurs via route 2 shown in Figure 4. On increasing the TEMPO concentration to 2 mg/mL, nearly 97% 5-HMF was converted in 2.5 h to yield over 80% FDCA, and continuing the reaction resulted in almost 100% of the 5-HMF being oxidized to give FDCA at >90% yield in 5.5 h. This corresponds to the incident photon-to-current efficiency of 9.29% and the Faradic efficiency of 92.6%. The earlier report using $BiVO_4$ photoelectrode revealed no oxidation of 5-HMF in the absence of TEMPO [5]. On the other hand, the high surface area nickel boride electrode providing

high current density of around 50 mA/cm^2 at a constant potential of 1.45 V_{RHE} (which is about six times higher than that in the present study) used for electrochemical oxidation showed 100% 5-HMF conversion to FDCA in just half an hour [20].

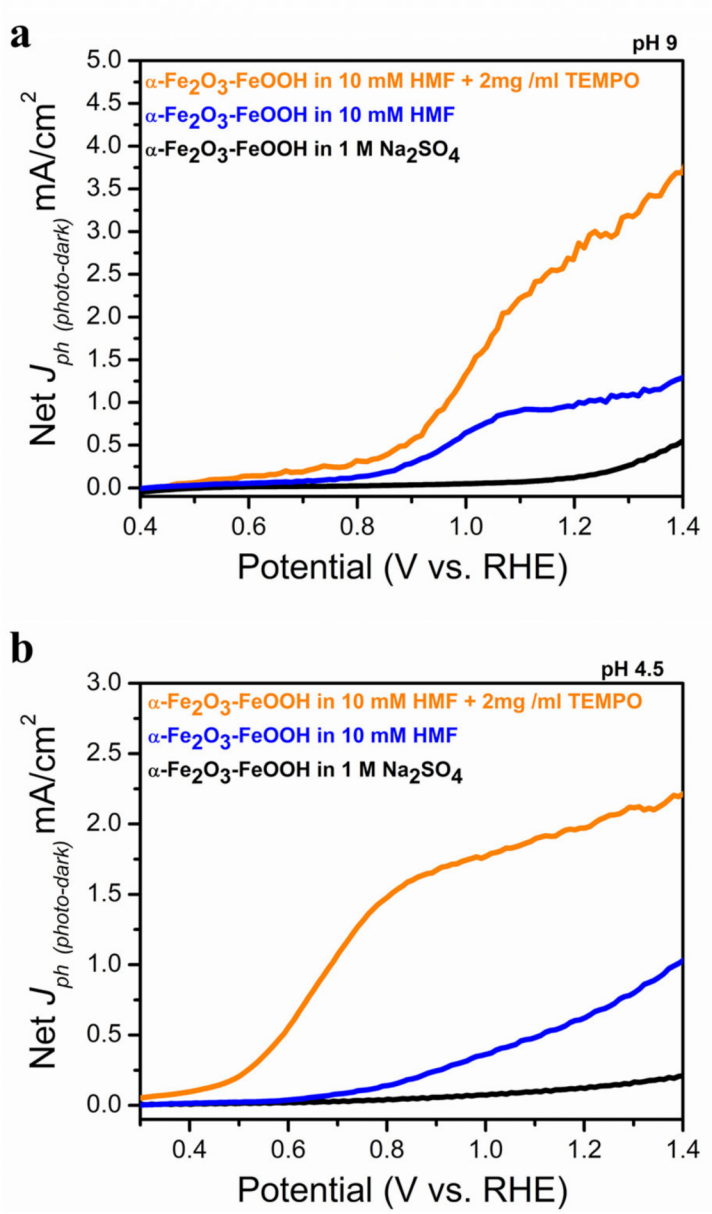

Figure 3. Net photocurrent responses for 5-HMF photooxidation at pH (**a**) 9.0 and (**b**) 4.5.

As seen in Table 1, the efficiency of oxidation decreases at lower pH values. At pH 9, 5-HMF was partially converted to a mixture of the route 1 intermediates 2,5-diformylfuran (DFF) and 5-formyl-2-furoic acid (FFCA) (Figure 4), the latter being present in a higher proportion. Reactions performed using FFCA, DFF, and HMFCA, respectively, as substrates under the same conditions showed DFF to be most efficiently converted with high selectivity to FFCA. On the other hand, HMFCA and FFCA were partly converted, but with high selectivity to FDCA. In all the experiments starting at pH 9.0, the pH was decreased to 5.0 (pH 6 in case of 5-HMFCA). The corresponding CA and current potential curves shown in Figures S5b–d and S6, respectively, indicate that the FFCA oxidation step is the slowest, in accordance with the previous report [5]. This corresponds to the incident photon-to-current efficiency of 6.07% and the Faradic efficiency of 12.6%.

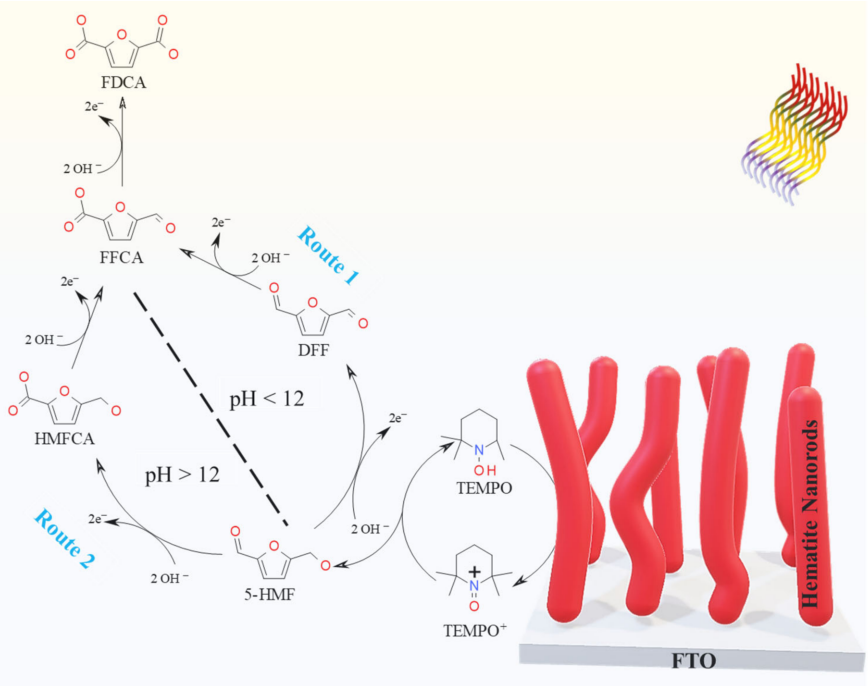

Figure 4. Schematic representation of the possible pathways of 5-HMF oxidation to FDCA at pH higher than 12.0 and pH less than 12.0.

5-HMF oxidation at pH 4.5 in the presence of 2 mg/mL TEMPO showed a similar pattern as at pH 9 (Figure 4), corresponding to the incident photon-to-current efficiency of 5.14% and the Faradic efficiency of 17.7%. The addition of the enzyme laccase (from *Trametes versicolor*) to the system significantly increased (78%) the degree of 5-HMF conversion, yielding FFCA as the main product. Laccases are multicopper oxidases found in plants, fungi, and bacteria, which catalyze the oxidation of phenolic and non-phenolic compounds while reducing oxygen to water [35]. The enzyme was not effective in the absence of TEMPO (Table 1).

The results obtained in this study are thus comparable to those in the earlier reports on photoelectrochemical oxidation of 5-HMF (Table S2). In the literature, three other PEC devices come closest to the efficiency we achieved in this study with a very inexpensive system. One device is a Ni/CdS nanosheet photoelectrode, which showed highly efficient oxidation of 5-HMF at the incredible power of 8W/cm^2 and operated at a significantly raised temperature (cost and necessary temperature control) [23]. This light intensity is an 80-fold increase to the typical solar irradiation of 100 mW/cm^2 used in this study. The second study uses CoPz/g-C_3N_4 under five times stronger illumination (500 mW/cm^2) and achieved 99.1% 5-HMF conversion at pH 9.18. This device operates at nearly 10 times lower 5-HMF concentration, significantly limiting the achievable conversion yields [19]. Closest to our system comes one reported device based upon a $BiVO_4$ electrode operated at elevated temperatures and functioning only in the presence of TEMPO [5]. In most studies, a higher operating temperature was suggested to play a critical role in the selective conversion of 5-HMF to FDCA. We highlight that our study is performed under ambient conditions, with a relatively higher concentration of 5-HMF (10 mM) and at the illumination power density of 100 mW/cm^2, representing the typical solar irradiation conditions.

In accordance with the report by Shuai et al. [19], it is evident that 5-HMF photooxidation using the modified hematite photoanode in the present study follows different routes depending on the pH of the electrolyte solution (Figure 4). It was indicated that a higher pH promotes the formation of alcohols and acids following the Cannizzaro mechanism, resulting in the two different pH-dependent mechanisms for 5-HMF oxidation. We also found that DFF and FFCA are unstable at higher pH, which is evident from the initial HPLC chromatograms shown in Figure S7.

As shown in Figure 4, with every oxidation step, two electrons are released in the solution (in total, six electrons) that are used in TEMPO regeneration. Considering that the reduction reaction at the counter electrode also plays a significant role in the photooxidation of 5-HMF, we believe that, at a low pH where the concentration of protons is comparatively higher, the FDCA yield is compensated by the reduction reaction at the cathode (H_2 generation). It would thus be important to study the 5-HMF oxidation in a dual-compartment cell separated by a Nafion membrane where both the oxidation and reduction reactions are separated to investigate the mass transfer limitations during 5-HMF photooxidation. It would also be interesting to study the reaction kinetics using recently developed in situ femtosecond transient absorption spectroscopy combined with spectroelectrochemistry techniques [36].

3. Experimental

3.1. Materials

Analytical-grade furan compounds FDCA, FFCA, DFF, and 5-HMF for use as HPLC standards (and in oxidation experiments in the case of FFCA and DFF), and the precursors ($FeCl_3$, $NaNO_3$, and NH_4F) for the synthesis of hematite photoanode, were purchased from Sigma Aldrich(Stockholm, Sweden). For use in oxidation experiments, 5-HMF and HMFCA were synthesized and purified in our laboratory at high purity according to our previous study [30]. (2,2,6,6-Tetramethylpiperidin-1-yl)oxyl (TEMPO) and *Trametes versicolor* laccase (specific activity of 0.5 U/mg) were purchased from Sigma Aldrich. Sodium sulfate and sodium hydroxide were purchased from Merck (Stockholm, Sweden). The photoelectrochemical (PEC) oxidation of the furan compounds was performed in a custom-made PEC cell. The Ag/AgCl reference electrode was purchased from IJ Cambria Scientific Ltd (Llanelli, UK). The potentiostat from PalmSens (Houten, The Netherlands) and Ivium Stat (Eindhoven, The Netherlands) was used for the PEC studies.

3.2. Hematite Photoanode Synthesis

The hematite photoanode was prepared following the method reported by Vayssieres and coworkers [27]. Briefly, 0.15 M ferric chloride and 1 M sodium nitrate solutions were adjusted to pH 1.1 by dropwise addition of 1 M HCl. The cleaned FTO substrates were immersed in this solution for 12 h and placed in an autoclave at a constant temperature of 100 °C. The FTO/α-Fe_2O_3 electrodes were then rinsed with distilled water and ethanol, followed by annealing at 800 °C for 5 min, and further modified by soaking in the fluoride-rich iron-oxide electrolyte (1 mM NH_4F in 0.15 M $FeCl_3$) for 5 h at 100 °C followed by rinsing with distilled water and subsequent annealing at 400 °C for 5 min to yield fluorine-doped FTO/α-Fe_2O_3/FeOOH.

3.3. Photoelectrochemical Oxidation of 5-HMF, HMFCA, FFCA, and DFF

A solution of 10 mM furan compounds, 5-HMF, DFF, HMFCA, and FFCA, respectively, was prepared in 50 mL of 1 M sodium sulfate (Na_2SO_4) with an average pH of 4.5. The furan solutions were also prepared with other pH values, 9 and 12, by adjusting pH using 1 M NaOH solution. Then, 30 mL of each solution, with respective pH values, was used directly or mixed with 1 or 2 mg/mL (2,2,6,6-Tetramethylpiperidin-1-yl)oxyl (TEMPO) in the photoelectrochemical cell for photooxidation at room temperature. Control experiments at different pH values were performed in dark while maintaining the other conditions.

The photoelectrode for the PEC measurements was prepared by gently polishing all the edges with sandpaper, and connected to the crocodile clip, and the assembly was sealed with conductive silver paste and further covered with Teflon tape. The other three edges were coated with insulating epoxy. The current potential curve, also called linear sweep voltammetry (LSV), was recorded for all the photoelectrodes in the dark and in light under various conditions used in this study. The cold-white LED (MCWHL6-C1, Thor Labs, Mölndal, Sweden) was used as a light source for illuminating the hematite photoanode. The illumination intensity was maintained at 100 mW/cm^2 throughout the study.

The LSVs were performed versus Ag/AgCl reference electrode and converted to reversible hydrogen electrode voltage using Equation (1):

$$V_{RHE} = V_{Ag/AgCl} + 0.1976 + (0.059 \times pH) \quad (1)$$

Moreover, photoelectrochemical oxidation of 5-HMF was performed using 1 mg/mL TEMPO at pH 12 as well as using 2 mg/mL TEMPO. The photoelectrochemical oxidation of 5-HMF at pH 9.0 and 4.5 was performed with and without 2 mg/mL TEMPO. At pH 4.5, we also tested the *T. versicolor* lacasse as the oxidation catalyst with and without TEMPO as the electron mediator. Five hundred microliter samples were collected at regular time intervals over the reaction time for HPLC analysis of the substrates, intermediates, and products.

3.4. Product Analysis

The concentrations of 5-HMF, FFA, FFCA, and FDCA were determined using HPLC (JASCO, Tokyo, Japan) equipped with a Bio-Rad Aminex HPX-87H column (connected to a guard column (Biorad, Richmond, CA, USA), refractive index detector (ERC, Kawaguchi, Japan), a JASCO UV detector operating at 254 nm, and a JASCO intelligent autosampler. The column temperature was maintained at 65 °C in a chromatographic oven (Shimadzu, Tokyo, Japan). Samples were diluted with Milli-Q quality water mixed with 20% (*v*/*v*) H_2SO_4 (20 µL/mL sample), and then filtered using 0.45 µm filter. A 40 µL aliquot was injected in 0.5 mM H_2SO_4 mobile phase flowing at a rate of 0.4 mL/min. The peaks for the different compounds were confirmed and quantified using the corresponding external standards.

The photoconversion of 5-HMF was calculated using Equation (2):

$$5-\text{HMF conversion } (\%) = \frac{(\text{Initial concentration} - \text{Final concentration})}{(\text{Initial concentration})} \times 100 \quad (2)$$

The yield (%) of the product formed was calculated using Equation (3):

$$\text{Yield of product } (\%) = \frac{(\text{mol of product formed })}{(\text{mol of initial } 5-\text{HMF})} \times 100 \quad (3)$$

The incident photon-to-current efficiency was calculated using Equation (4)

$$IPCE = \frac{(|j|) \times 1239.8}{P \times \lambda} \times 100 \quad (4)$$

where 1239.8 V nm represents a multiplication of h (Planck's constant) and c (the speed of light), P is the calibrated and monochromated illumination power density in mW/cm^2, and λ is the illumination wavelength.

The Faradic efficiency based on the 5-HMF conversion into products was calculated using Equation (5).

$$FE\ (\%) = \frac{mol\ of\ HMF\ Converted}{total\ charge\ passed} \times n \times F \times 100 \quad (5)$$

where n is the number of electrons transferred during 5-HMF oxidation ($6e^-$) and F is the Faraday constant 96,485.3 s A mol^{-1}.

4. Conclusions

In conclusion, this study demonstrates 99.2% 5-HMF conversion to FDCA with a yield of >90% using hematite photoelectrode under visible illumination at pH > 12, ambient temperature (21 ± 1 °C), and atmospheric pressure in the presence of TEMPO. The 5-HMF oxidation follows different routes at pH above and below 12, i.e., via HMFCA and DFF, respectively. The rate-limiting steps in the respective cases are the oxidation of HMFCA and FFCA. Besides FDCA, even the intermediate oxidation products HMFCA, DFF, and FFCA bearing different functionalities (hydroxyl, aldehyde, and carboxyl), formed

during the PEC oxidation, constitute highly interesting building blocks for novel polymer structures. This study serves as the foundation for the photo-conversion of 5-HMF that can be enhanced in the future for selective production of FDCA by synthesizing high surface area Earth-abundant hematite photoelectrodes and subsequent modification with a suitable dopant. As is well known, the large-scale application of TEMPO is limited by its high cost and potential toxicity. It would thus be important to consider alternative strategies including polymer-supported TEMPO to enable its recycling and/or using other electron mediators that are less expensive like TEMPOL (4-hydroxy-TEMPO) or those based on natural resources like sinapic acid and syringaldehyde [34,37–41].

Supplementary Materials: The following are available online at https://www.mdpi.com/article/10.3390/catal11080969/s1, Figure S1 (a) X-ray diffraction patterns for the bare (black trace) and modified hematite (red trace); (b) and (c) show the planar top view scanning electron micrograph for bare and modified hematite photoanode, respectively, before the PEC experiment; while (d) shows a planar top view scanning electron micrograph after the 20 h PEC run. The bar represents 1 μm. The bar represents 1 μm. Figure S2 LSVs for the bare and modified hematite photoanodes at different pH values (4.5, 9.0, and 12.5) in 1 M Na_2SO_4 solution, and the corresponding dark current for (c) bare and (d) modified photoanodes, respectively. The dark current response for 5-HMF oxidation at (e) pH 12.5, (f) 9.0, and (g) 4.5 are also shown. Table S1 V_{onset} potentials obtained for modified hematite under different pH conditions and the net photocurrent density recorded at 1.4 V_{RHE} (in square bracket, orange color). Figure S3 Cyclic voltammograms recorded in Na_2SO_4 + TEMPO with and without 5-HMF in dark and under illumination at pH (a) 12.5, (b) pH 9.0, and (c) pH 4.5. Figure S4 Chronoamperometry response for 5-HMF oxidation recorded under visible illumination and 1.1 V_{RHE} at 100 mW/cm^2 for α-Fe_2O_3-FeOOH in 1 M Na_2SO_4 solution at pH 4.5. Figure S5 Chronoamperometry response for (a) 5-HMF, (b) FFCA, (c) HMFCA, and (d) DFF oxidation recorded under visible illumination and 1.1 V_{RHE} at 100 mW/cm^2 for α-Fe_2O_3-FeOOH in 1 M Na_2SO_4 solution (pH 9.0). Figure S6 LSVs for the modified hematite photoanode recorded for different furan compounds as substrates at pH 9.0 in 1 M Na_2SO_4 solution. Figure S7 HPLC chromatograms of the photooxidation of (a) DFF, (b) HMFCA, and (c) FFCA in 1M Na_2SO_4 solution at pH 12.5 with 2 mg/mL TEMPO. Table S2 Comparison of the system presented in this study with other photoelectrochemical or photocatalytic systems reported in the literature on 5-HMF oxidation to FDCA.

Author Contributions: A.K., M.S., and R.H.-K. conceptualized the project. A.K., M.S., T.P., and R.H.-K. designed the experiments. A.K. prepared the photoelectrodes and performed the PEC. measurements. M.S. prepared the furan compounds for the study and performed the HPLC analyses. Q.S. performed the XRD on the photoanode samples. J.U. helped with the chronoamperometry and PEC instrumentation setup and revising the manuscript. A.K. and R.H.-K. wrote the manuscript with important inputs from the co-authors. T.P. and R.H.-K. provided the resources, supervision, arranged funding, and project administration. All authors have read and agreed to the published version of the manuscript.

Funding: T.P. acknowledges financial support from Swedish Energy Agency (grant no. 50709-1 and 44651-1) and Swedish Research Council (grant no. 2018-05090). R.H.-K. acknowledges financial support from the Swedish Foundation for Strategic Environmental Research (Mistra, grant no. 2016/1489), Swedish Research Agency Formas (grant no. 942-2016-33), and Lantmännen Research Foundation (grant no. 2019H045).

Data Availability Statement: The data shown in this paper are available upon request.

Acknowledgments: A.K. acknowledges assistance from NanoLund cleanroom facilities for the synthesis of photoelectrodes.

Conflicts of Interest: The authors declare no competing financial interest.

References

1. Chemicals. Available online: https://www.iea.org/fuels-and-technologies/chemicals (accessed on 1 June 2021).
2. Davidson, M.G.; Elgie, S.; Parsons, S.; Young, T.J. Production of HMF, FDCA and their derived products: A review of life cycle assessment (LCA) and techno-economic analysis (TEA) studies. *Green Chem.* **2021**, *23*, 3154–3171. [CrossRef]
3. Gratzel, M. Photoelectrochemical cells. *Nature* **2001**, *414*, 338–345. [CrossRef]
4. Vennestrøm, P.; Osmundsen, C.M.; Christensen, C.; Taarning, E. Beyond petrochemicals: The renewable chemicals industry. *Angew. Chem. Int. Ed.* **2011**, *50*, 10502–10509. [CrossRef]
5. Cha, H.G.; Choi, K.-S. Combined biomass valorization and hydrogen production in a photoelectrochemical cell. *Nat. Chem.* **2015**, *7*, 328. [CrossRef] [PubMed]
6. Lianos, P. Production of electricity and hydrogen by photocatalytic degradation of organic wastes in a photoelectrochemical cell: The concept of the photofuelcell: A review of a re-emerging research field. *J. Hazard. Mater.* **2011**, *185*, 575–590. [CrossRef] [PubMed]
7. Roger, I.; Shipman, M.A.; Symes, M.D. Earth-abundant catalysts for electrochemical and photoelectrochemical water splitting. *Nat. Rev. Chem.* **2017**, *1*, 3. [CrossRef]
8. Lhermitte, C.R.; Sivula, K. Alternative oxidation reactions for solar-driven fuel production. *ACS Catal.* **2019**, *9*, 2007–2017. [CrossRef]
9. Kawde, A.; Annamalai, A.; Amidani, L.; Boniolo, M.; Kwong, W.L.; Sellstedt, A.; Glatzel, P.; Wågberg, T.; Messinger, J. Photo-electrochemical hydrogen production from neutral phosphate buffer and seawater using micro-structured p-Si photo-electrodes functionalized by solution-based methods. *Sustain. Energy Fuels* **2018**, *2*, 2215–2223. [CrossRef]
10. Kawde, A.; Annamalai, A.; Sellstedt, A.; Uhlig, J.; Wågberg, T.; Glatzel, P.; Messinger, J. More than protection: The function of TiO_2 interlayers in hematite functionalized Si photoanodes. *Phys. Chem. Chem. Phys.* **2020**, *22*, 28459–28467. [CrossRef] [PubMed]
11. Kawde, A.; Annamalai, A.; Sellstedt, A.; Glatzel, P.; Wågberg, T.; Messinger, J. A microstructured p-Si photocathode outcompetes Pt as a counter electrode to hematite in photoelectrochemical water splitting. *Dalton Trans.* **2019**, *48*, 1166–1170. [CrossRef]
12. Luo, J.; Steier, L.; Son, M.-K.; Schreier, M.; Mayer, M.T.; Graätzel, M. Cu_2O nanowire photocathodes for efficient and durable solar water splitting. *Nano Lett.* **2016**, *16*, 1848–1857. [CrossRef]
13. Liang, Y.; Messinger, J. Improving $BiVO_4$ photoanodes for solar water splitting through surface passivation. *Phys. Chem. Chem. Phys.* **2014**, *16*, 12014–12020. [CrossRef]
14. Werpy, T.; Petersen, G. *Top Value Added Chemicals from Biomass: Volume I–Results of Screening for Potential Candidates from Sugars and Synthesis Gas*; National Renewable Energy Lab.: Golden, CO, USA, 2004.
15. Román-Leshkov, Y.; Chheda, J.N.; Dumesic, J.A. Phase modifiers promote efficient production of hydroxymethylfurfural from fructose. *Science* **2006**, *312*, 1933–1937. [CrossRef]
16. Jacquel, N.; Saint-Loup, R.; Pascault, J.-P.; Rousseau, A.; Fenouillot, F. Bio-based alternatives in the synthesis of aliphatic–aromatic polyesters dedicated to biodegradable film applications. *Polymer* **2015**, *59*, 234–242. [CrossRef]
17. Davis, S.E.; Houk, L.R.; Tamargo, E.C.; Datye, A.K.; Davis, R.J. Oxidation of 5-hydroxymethylfurfural over supported Pt, Pd and Au catalysts. *Catal. Today* **2011**, *160*, 55–60. [CrossRef]
18. Liguori, F.; Barbaro, P.; Calisi, N. Continuous-Flow Oxidation of HMF to FDCA by Resin-Supported Platinum Catalysts in Neat Water. *ChemSusChem* **2019**, *12*, 2558–2563. [CrossRef]
19. Xu, S.; Zhou, P.; Zhang, Z.; Yang, C.; Zhang, B.; Deng, K.; Bottle, S.; Zhu, H. Selective oxidation of 5-hydroxymethylfurfural to 2, 5-furandicarboxylic acid using O_2 and a photocatalyst of Co-thioporphyrazine bonded to g-C3N4. *J. Am. Chem. Soc.* **2017**, *139*, 14775–14782. [CrossRef]
20. Barwe, S.; Weidner, J.; Cychy, S.; Morales, D.M.; Dieckhöfer, S.; Hiltrop, D.; Masa, J.; Muhler, M.; Schuhmann, W. Electrocatalytic Oxidation of 5-(Hydroxymethyl) furfural Using High-Surface-Area Nickel Boride. *Angew. Chem. Int. Ed.* **2018**, *57*, 11460–11464. [CrossRef]
21. Mi, Q.; Zhanaidarova, A.; Brunschwig, B.S.; Gray, H.B.; Lewis, N.S. A quantitative assessment of the competition between water and anion oxidation at WO 3 photoanodes in acidic aqueous electrolytes. *Energy Environ. Sci.* **2012**, *5*, 5694–5700. [CrossRef]
22. Fuku, K.; Wang, N.; Miseki, Y.; Funaki, T.; Sayama, K. Photoelectrochemical Reaction for the Efficient Production of Hydrogen and High-Value-Added Oxidation Reagents. *ChemSusChem* **2015**, *8*, 1593–1600. [CrossRef]
23. Han, G.; Jin, Y.-H.; Burgess, R.A.; Dickenson, N.E.; Cao, X.-M.; Sun, Y. Visible-light-driven valorization of biomass intermediates integrated with H2 production catalyzed by ultrathin Ni/CdS nanosheets. *J. Am. Chem. Soc.* **2017**, *139*, 15584–15587. [CrossRef] [PubMed]
24. Chen, Z.; Dinh, H.N.; Miller, E. *Photoelectrochemical Water Splitting*; Springer: New York, NY, USA, 2013; Volume 344, ISBN 978-1-4614-8297-0.
25. Vuyyuru, K.R.; Strasser, P. Oxidation of biomass derived 5-hydroxymethylfurfural using heterogeneous and electrochemical catalysis. *Catal. Today* **2012**, *195*, 144–154. [CrossRef]
26. Kim, J.Y.; Jang, J.W.; Youn, D.H.; Magesh, G.; Lee, J.S. A stable and efficient hematite photoanode in a neutral electrolyte for solar water splitting: Towards stability engineering. *Adv. Energy Mater.* **2014**, *4*, 1400476. [CrossRef]
27. Vayssieres, L.; Beermann, N.; Lindquist, S.-E.; Hagfeldt, A. Controlled aqueous chemical growth of oriented three-dimensional crystalline nanorod arrays: Application to iron (III) oxides. *Chem. Mater.* **2001**, *13*, 233–235. [CrossRef]
28. Kormányos, A.; Kecsenovity, E.; Honarfar, A.; Pullerits, T.; Janáky, C. Hybrid FeNiOOH/α-Fe_2O_3/Graphene Photoelectrodes with Advanced Water Oxidation Performance. *Adv. Funct. Mater.* **2020**, *30*, 2002124. [CrossRef]

29. Wang, T.; Long, X.; Wei, S.; Wang, P.; Wang, C.; Jin, J.; Hu, G. Boosting Hole Transfer in the Fluorine-Doped Hematite Photoanode by Depositing Ultrathin Amorphous FeOOH/CoOOH Cocatalysts. *ACS Appl. Mater. Interfaces* **2020**, *12*, 49705–49712. [CrossRef]
30. Sayed, M.; Warlin, N.; Hulteberg, C.; Munslow, I.; Lundmark, S.; Pajalic, O.; Tunå, P.; Zhang, B.; Pyo, S.-H.; Hatti-Kaul, R. 5-Hydroxymethylfurfural from fructose: An efficient continuous process in a water-dimethyl carbonate biphasic system with high yield product recovery. *Green Chem.* **2020**, *22*, 5402–5413. [CrossRef]
31. Bragd, P.; Van Bekkum, H.; Besemer, A. TEMPO-mediated oxidation of polysaccharides: Survey of methods and applications. *Top. Catal.* **2004**, *27*, 49–66. [CrossRef]
32. Sivula, K.; Le Formal, F.; Grätzel, M. Solar water splitting: Progress using hematite (α-Fe_2O_3) photoelectrodes. *ChemSusChem* **2011**, *4*, 432–449. [CrossRef]
33. Annamalai, A.; Shinde, P.S.; Subramanian, A.; Kim, J.Y.; Kim, J.H.; Choi, S.H.; Lee, J.S.; Jang, J.S. Bifunctional TiO_2 underlayer for α-Fe_2O_3 nanorod based photoelectrochemical cells: Enhanced interface and Ti^{4+} doping. *J. Mater. Chem. A* **2015**, *3*, 5007–5013. [CrossRef]
34. Gerken, J.B.; Pang, Y.Q.; Lauber, M.B.; Stahl, S.S. Structural Effects on the pH-Dependent Redox Properties of Organic Nitroxyls: Pourbaix Diagrams for TEMPO, ABNO, and Three TEMPO Analogs. *J. Org. Chem.* **2017**, *83*, 7323–7330. [CrossRef] [PubMed]
35. Riva, S. Laccases: Blue enzymes for green chemistry. *TRENDS Biotechnol.* **2006**, *24*, 219–226. [CrossRef]
36. Honarfar, A.; Mourad, H.; Lin, W.; Polukeev, A.; Rahaman, A.; Abdellah, M.; Chábera, P.; Pankratova, G.; Gorton, L.; Zheng, K. Photoexcitation Dynamics in Electrochemically Charged CdSe Quantum Dots: From Hot Carrier Cooling to Auger Recombination of Negative Trions. *ACS Appl. Energy Mater.* **2020**, *3*, 12525–12531. [CrossRef]
37. Ciriminna, R.; Pagliaro, M. Industrial oxidations with organocatalyst TEMPO and its derivatives. *Org. Process Res. Dev.* **2010**, *14*, 245–251. [CrossRef]
38. Dijksman, A.; Arends, I.W.; Sheldon, R.A. Polymer immobilised TEMPO (PIPO): An efficient catalyst for the chlorinated hydrocarbon solvent-free and bromide-free oxidation of alcohols with hypochlorite. *Chem. Commun.* **2000**, *66*, 271–272. [CrossRef]
39. Liu, S.; Liang, H.; Sun, T.; Yang, D.; Cao, M. A recoverable dendritic polyamidoamine immobilized TEMPO for efficient catalytic oxidation of cellulose. *Carbohydr. Polym.* **2018**, *202*, 563–570. [CrossRef]
40. Mani, P.; Fidal Kumar, V.T.; Keshavarz, T.; Chandra, T.S.; Kyazze, G. The role of natural laccase redox mediators in simultaneous dye decolorization and power production in microbial fuel cells. *Energies* **2018**, *11*, 3455. [CrossRef]
41. Zhang, K.; Wu, Y.; Huang, J.; Liu, Y. Environmentally Friendly and Recyclable Natural-Mediator-Modified Magnetic Nanoparticles for Laccase-Catalyzed Decolorization. *J. Chem.* **2019**, *2019*, 4140565. [CrossRef]